The EMBO Journal Vol. 20 No. 6 pp. 1310–1319, 2001

Adenovirus-activated PKA and p38/MAPK pathways boost microtubule-mediated nuclear targeting of virus

M.Suomalainen[1], M.Y.Nakano, K.Boucke, S.Keller and U.F.Greber[2]

University of Zürich, Institute of Zoology, Winterthurerstrasse 190, CH-8057 Zürich, Switzerland

[1]Present address: Karolinska Institute, Department of Biosciences at Novum, S-141 57 Huddinge, Sweden

[2]Corresponding author
e-mail: ufgreber@zool.unizh.ch

M.Suomalainen and M.Y.Nakano contributed equally to this work

Nuclear targeting of adenovirus is mediated by the microtubule-dependent, minus-end-directed motor complex dynein/dynactin, in competition with plus-end-directed motility. We demonstrate that adenovirus transiently activates two distinct signaling pathways to enhance nuclear targeting. The first pathway activates integrins and cAMP-dependent protein kinase A (PKA). The second pathway activates the p38/MAP kinase and the downstream MAPKAP kinase 2 (MK2), dependent on the p38/MAPK kinase MKK6, but independent of integrins and PKA. Motility measurements in PKA-inhibited, p38-inhibited or MK2-lacking ($MK2^{-/-}$) cells indicate that PKA and p38 stimulated both the frequency and velocity of minus-end-directed viral motility without affecting the perinuclear localization of transferrin-containing endosomal vesicles. p38 also suppressed lateral viral motilities and MK2 boosted the frequency of minus-end-directed virus transport. Nuclear targeting of adenovirus was rescued in $MK2^{-/-}$ cells by overexpression of hsp27, an MK2 target that enhances actin metabolism. Our results demonstrate that complementary activities of PKA, p38 and MK2 tip the transport balance of adenovirus towards the nucleus and thus enhance infection.

Keywords: adenovirus/MAPK/microtubules/PKA/regulated nuclear targeting

Introduction

Eukaryotic cells have two principal mechanisms of intracellular motility: microtubule- and actin filament-based systems and their associated motor proteins. Microtubules have been proposed to serve as tracks for long-range transport of organelles and pathogens either towards or away from the cell center (Sheetz, 1999). Actin filaments seem to support local organelle transport preferentially. Both of these motility systems are exploited by intracellular pathogens (Dramsi and Cossart, 1998; Frischknecht *et al*., 1999; Sodeik, 2000). Adenovirus (Ad), which replicates in the cell nucleus, is an example of a pathogen that traverses the cytoplasm by microtubule-mediated motility when entering into a new host cell (Suomalainen *et al*., 1999; Leopold *et al*., 2000). Cytosolic Ad particles engage in both minus- and plus-end-directed motilities along stable microtubules. Minus-end-directed motions are mediated by the dynein/dynactin motor complex, but the plus-end-directed motor remains to be characterized. Switching between minus- and plus-end-directed motions occurs frequently. In model cell lines like HeLa and TC7, the minus-end-directed motility is dominant, causing net movement of particles towards the perinuclear microtubule organizing center and the nucleus at population speeds in the order of micrometers per minute (Suomalainen *et al*., 1999). At present, it is unknown how the balance between minus- and plus-end-directed motions is maintained.

Signal transduction is emerging as an important regulator of early virus–host interactions. Two basic mechanisms account for virus-induced cell signaling: the activation of surface receptor(s) during lytic or non-lytic replication and the deposition of signaling molecules into a target cell. Activation of viral receptors can stimulate or counteract cellular antiviral defenses, enhance apoptosis or facilitate virus entry and production (Pelchen-Matthews *et al*., 1999; Wallach *et al*., 1999; Griego *et al*., 2000; Krijnse Locker *et al*., 2000). Similarly, the delivery of activated MAPK by incoming HIV-1 seems to facilitate early step(s) of virus infection (Jacque *et al*., 1998).

Studies on Ad support the importance of cell signaling in virus entry. Ad2 or Ad5 initially docks to the immunoglobulin gene family receptor CAR (Coxsackie B virus adenovirus receptor; Bergelson *et al*., 1997) and initiates infection in the absence of the cytosolic and membrane-spanning CAR domains (Wang and Bergelson, 1999). Viral interactions with $\alpha_v\beta_5$ integrins activate the lipid kinase PI3K, the small G proteins cdc42 and rac1, and trigger endocytosis (Nemerow and Stewart, 1999). Virus escapes to the cytosol by causing disruption of endocytic vesicles, and the particle then engages in bidirectional movement along microtubules (Suomalainen *et al*., 1999). Here we show that incoming Ad2 triggers two distinct signaling pathways, which increase cytosolic motility and boost minus-end-directed motions of viral particles along microtubules. The upregulated signaling pathways are necessary for efficient delivery of viral genome to the nucleus.

Results

Cytosolic Ads have two types of motility: bidirectional microtubule-dependent long-range motility and short-range microtubule-independent lateral motion.

We first asked whether incoming Ad2 signals to the host cell stimulate motilities of cytosolic particles. Texas red-labeled intact Ad2 (Ad2–TR) particles were microinjected

into HeLa cells. Prior to injection, virus binding sites at the cell surface were saturated with an excess of soluble fiber knob fragments to preclude natural infections (Louis *et al*., 1994; Nakano and Greber, 2000). Cells were imaged in live fluorescence mode and individual viral particles traced at 15–70 min post-injection. Microinjected Ad2 particles showed homogeneous motilities at low levels. Vectorial velocities of elementary motion steps (ES; movement of a particle between two subsequent frames) were center directed (v_c), periphery directed (v_p) or directed to lateral sides (v_l) and reached levels of 0.11–0.12 μm/s, giving a population velocity of –0.05 μm/min towards the nucleus (Figure 1A). The motility frequency (% ES >0.1 μm/s) was 20%. Challenging the injected cells by an infection with unlabeled Ad2 before adding fiber knobs increased the overall motility frequency of the fluorescent particles to 52% (Figure 1B). The challenge also significantly increased (p <0.01) the three vectorial ES components to 0.16–0.17 μm/s and shifted the population velocity to 0.21 μm/min towards the periphery. Stimulated motilities were not dependent on microtubule treadmilling and dynamic instability since stabilization of microtubules with taxol had no effect on viral motilities (not shown). Complete disruption of the microtubule network by combined cold and nocodazole (noc) treatments reduced the population velocity to 0.03 μm/min and the motility frequency to 8%, and also diminished v_p, v_l and v_c (p <0.01; Figure 1C). Taken together, these results indicate that a wild-type infection predominantly stimulated microtubule-dependent motilities of intact cytosolic virus particles.

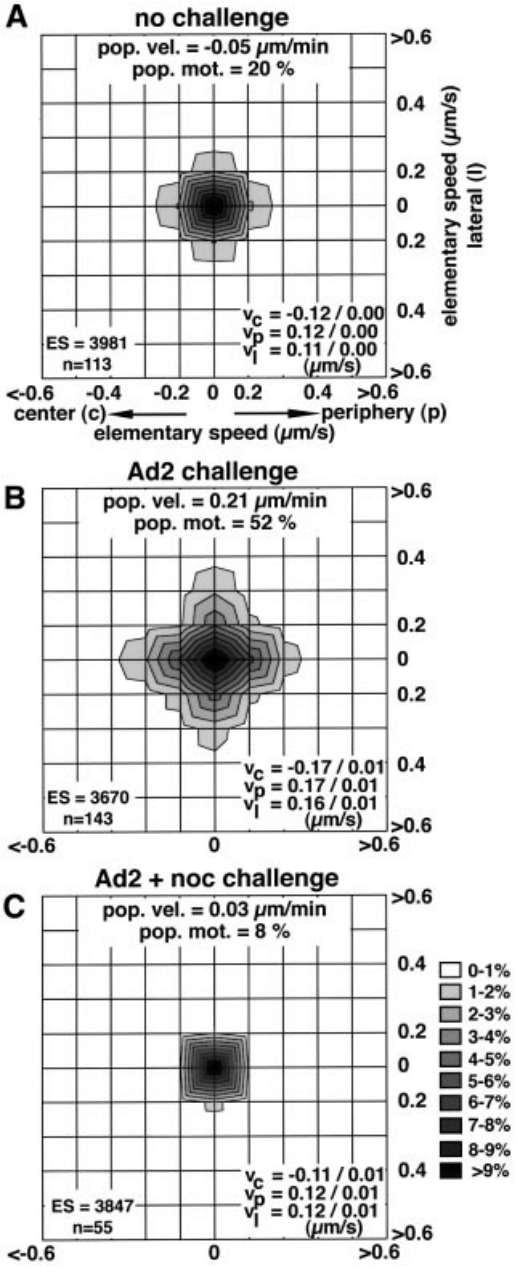

Fig. 1. Ad2 infection stimulates microtubule-dependent motility of cytosolic microinjected Ad2 particles. Microinjected Ad2–TR was analyzed by time-lapse fluorescence microscopy and ES were analyzed for each particle (n) in control HeLa cells (**A**), HeLa cells challenged with a normal Ad2 infection (**B**) or with Ad2 plus nocodazole (**C**). Population velocities, population motilities, average vectorial velocities to the center (v_c), the periphery (v_p) and lateral directions (v_l) were determined based on the number of ES from n particles. Supplementary animation is available at *The EMBO Journal* Online.

Ad-induced PKA activity required for nuclear targeting

Intracellular cAMP levels regulate microtubule-dependent transport of melanosomes in fish and amphibian chromatophores (Reilein *et al*., 1998; Reese and Haimo, 2000). We therefore tested whether interference with cAMP-dependent protein kinase (PKA) activity affected nuclear accumulation of incoming Ad2. HeLa cells were pretreated with a cell-permeable specific peptidic inhibitor of PKA (PKI-myr at 55 μM; Gamm and Uhler, 1995). The subcellular localization of Ad2–TR was visualized by confocal laser scanning microscopy (CLSM) at 70 min post-infection (p.i.). Control untreated cells enriched Ad2–TR in the cell center (Figure 2A, a) coincident with the nucleus (not shown), whereas PKA-inhibited cells contained many virus particles near the cell periphery (Figure 2A, b, arrows). Quantitative fluorescence microscopy demonstrated that PKI-myr-treated cells contained significantly more virus fluorescence near the periphery and in the cytoplasmic area than control cells or cells treated with a control myristoylated peptide, autocamptide (80 μM), an inhibitor of calcium/calmodulin-dependent kinase II (p <0.01; Figure 2B). Conversely, PKI-myr-treated cells failed to enrich Ad2 at the nucleus (p <0.01) and the perinuclear region (not shown). Viral DNA was found at reduced levels in the nucleoplasm of PKI-myr-treated cells (Figure 2A, c and d). Other PKA inhibitors, such as KT5720 (5 μM) and H89 (40 μM), which are directed to the ATP binding site, gave similar results (not shown). The PKI-myr effects on Ad2 localization were largely reversible by washing out the inhibitor and stimulating PKA activity with forskolin and the diesterase inhibitor isobutyl methylxanthine (IBMX) for 60 min (p <0.01; Figure 2B). Washing out the inhibitor without PKA stimulation was not effective (not shown), suggesting that efficient nuclear targeting of Ad2 requires stimulated PKA.

We tested whether incoming Ad2 activated cellular PKA. Virus was bound to HeLa cells in the cold and cells

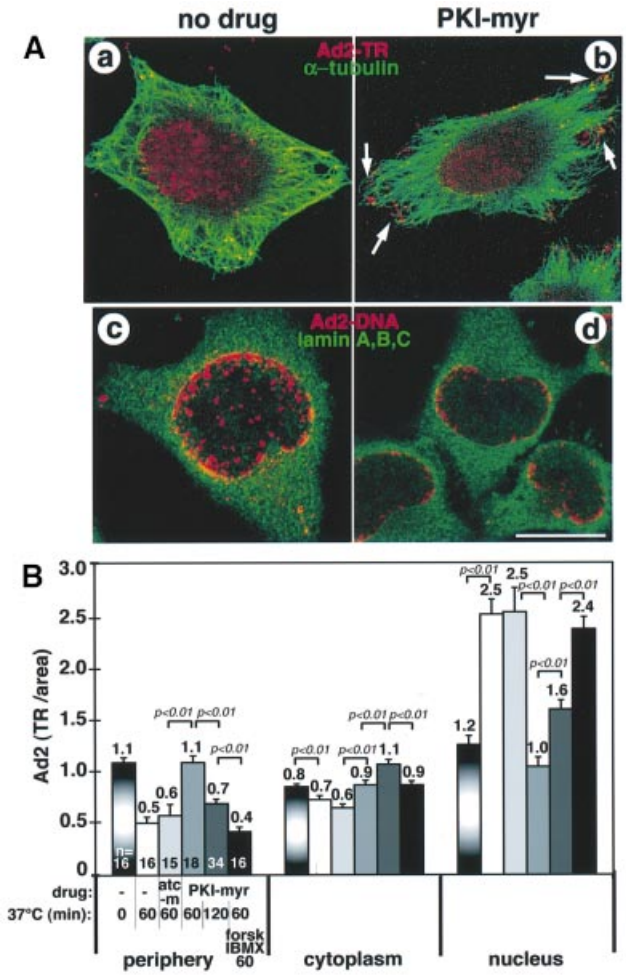

Fig. 2. Nuclear targeting and DNA import of Ad2 are blocked by PKA inhibitors. (**A**) Control or PKI-myr-treated HeLa cells were infected with Ad2–TR for 70 min (a and b, red) or with unlabeled Ad2 for 180 min (c and d), fixed and processed for tubulin staining (a and b, green) or for FISH analysis of viral DNA (red) using lamins A, B, C (green) as nuclear envelope markers (c and d). The entire stack of Ad2–TR images is shown in (a) and (b). Three merged optical sections from comparable z-regions of the cells are shown for viral DNA (c and d). Clustering of Ad2–TR in the periphery of PKI-myr-treated cells is highlighted by arrows. Note the cytoplasmic background staining of the lamins in the FISH assays (c and d). Scale bar = 10 μm. (**B**) Quantification of the subcellular localization of Ad2–TR. Control cells and cells pre-treated with PKI-myr or myristoylated autocamptide (atc-m) were infected with Ad2–TR for 0, 60 or 120 min, followed by washout of PKI-myr and subsequent incubation in drug-free medium containing forskolin (forsk) and IBMX as indicated. The mean values of TR fluorescence in the cell periphery, the cytoplasm and the nuclear areas are indicated, including the SEM, *p* values and the number of cells analyzed (*n*).

were infected at 37°C for different times. PKA activity was determined using the kemptide assay and kinase activity expressed as a percentage of the total PKA activity measured in the presence of cAMP. In Ad2-infected cells, we have observed a consistent, transient ~3.5-fold upregulation of kemptide phosphorylation, which peaked at 15–30 min p.i. (Figure 3A). This activity was largely due to stimulation of PKA, since the specific PKA inhibitor PKIα or a pre-treatment of cells with the cell-permeable inhibitor H89 (40 μM) strongly reduced virus-induced kemptide phosphorylation (Figure 3B and C). The Ad2-induced kinase activity amounted to ~3% of the total cellular PKA activity and was comparable to forskolin induction (Figure 3B). Forskolin- but not virus-induced activity was further boosted by the diesterase inhibitor IBMX. Stimulation of PKA activity depended on the amount of input virus. A reliable readout was obtained at ~10^4 particles per cell and peaked at 10^5 particles per cell (Figure 3C). Using radiolabeled Ad2, we estimated that under these conditions ~2% of input particles actually bound to the cells, thus suggesting that a few hundred virus particles per cell were sufficient to allow PKA measurements. Importantly, binding and internalization of the non-infectious Ad2 mutant ts1 did not stimulate PKA, suggesting that wild-type virus stimulated cellular PKA levels rather than imported the activity into the cell (Figure 3C). Accordingly, we did not detect any PKA activity in purified Ad2 particles (data not shown). Activation of PKA required Ad2 contacts to surface integrins since blocking of these contacts by cRGD (cyclic arginine-glycine-aspartate) peptides (0.2 mM) or treatment of cells with low Ca^{2+} medium inhibited PKA stimulation (Figure 3D). Since cRGD or low Ca^{2+} medium also inhibits virus uptake and penetration into the cytoplasm (Greber *et al*., 1997; Nemerow and Stewart, 1999), it was possible that some downstream event, rather than virus interaction with integrins, was required for PKA activation. However, this is unlikely since calphostin (1 μM), which targets protein kinase C and inhibits virus escape from endosomes (Nakano *et al*., 2000), had no effect on PKA activation (Figure 3D). Similarly, noc treatment of cells only moderately reduced PKA activation (Figure 3D). Collectively, these observations show that incoming Ad2 transiently activates PKA by contacting cell surface integrins. This stimulation sets the stage for effective nuclear translocation of the incoming virus particles.

Activation of p38/MAPK but not ERK1,2 is needed for nuclear targeting of Ad2

Incoming Ad5 upregulates the Raf/MAPK signaling pathway 15–20 min p.i., leading to a delayed production of interleukin (IL)-8 (Bruder and Kovesdi, 1997). We first tested whether activation of ERK1,2 was required for nuclear transport of Ad2 by infecting HeLa cells in the presence or absence of the MAPK kinase (MEK1) inhibitor PD98059 (PD; 20 μM; Alessi *et al*., 1995). Although PD completely eliminated activated ERK1,2 (Figure 5E), nuclear transport of Ad2 was unaffected in PD-treated cells (Figure 4A, e and f), demonstrating that activation of the MEK/ERK1,2 pathway was not required for virus entry. Accordingly, PD had no effect on the activation of PKA, indicating that MEK and ERK did not activate PKA in Ad2-infected cells (Figure 3D).

Viral infections commonly induce cellular stress pathways (Miller and Raab-Traub, 1999; Tang *et al*., 1999). Recent results suggested that stress activation is linked to microtubule-dependent motor function (Nagata *et al*., 1998; De Vos *et al*., 2000). To determine whether the stress-activated p38/MAPK pathway affected nuclear transport of Ad2 we treated cells with SB203580 (SB; 10 μM), a specific inhibitor of the α,β isoforms of p38/MAPK (Beyaert *et al*., 1996). Analysis of Ad2–TR fluorescence by CLSM and quantitative fluorescence

microscopy indicated that nuclear targeting of Ad2 was inhibited in SB-treated cells (Figure 4A and B). Cells treated with SB202474, a pyridinyl imidazole related to SB but inactive on p38 (Lee *et al*., 1994), had a slightly reduced nuclear targeting index of 2.9, compared with 3.4 for control and 1.3 for SB-treated cells (not shown). Importantly, the perinuclear localization of internalized transferrin was not affected by the p38 inhibitor SB, indicating that p38 was specifically required for intracellular targeting of Ad2 but not for microtubule-dependent endosomal transport (Figure 4A, b and d). SB treatment increased the levels of virus particles in the periphery and the cytoplasm at 90 and 140 min p.i., compared with control cells ($p = 0.025$ and $p < 0.01$), and decreased virus fluorescence near the nucleus ($p < 0.01$; Figure 4B) and the perinuclear region (not shown). This inhibition was partially reversed by SB washout and p38 stimulation by sorbitol (see Raingeaud *et al*., 1996). Drug washout without sorbitol was not effective, suggesting that p38 induction was crucial for nuclear targeting of Ad2 (not shown). Whether p38 activation was in fact required for Ad2 nuclear targeting was tested by transient transfection of dominant-negative (dn) MKK6(K82A) (Figure 4C). p38 is a major target of MKK6 and not activated in the presence of dn MKK6 (Raingeaud *et al*., 1996). MKK6(K82A) or constitutively active MKK6(EE207/211), but not constitutively active MEK1(EE217/221) or eGFP alone (not shown), blocked nuclear and perinuclear targeting of Ad2, and increased the levels of peripheral ($p < 0.01$) and cytoplasmic virus (compared with non-transfected control cells of Figure 4B). The observation that constitutively active MKK6 was apparently a slightly better inhibitor of nuclear (but not perinuclear) targeting of Ad2 was most likely due to cell elongation (spindle-like shape) by MKK6(K82A) overexpression, rather than a real difference in nuclear accumulation (not shown). Importantly, overexpression of the phosphorylation-defective dn p38 (T180A, Y182F) also blocked Ad2 nuclear targeting (not shown). Collectively, the results indicated that p38 stimulation by MKK6 is required for Ad2 nuclear targeting.

Stimulation of the p38 pathway by inflammatory cytokines or stress conditions activates the p38 target MAPKAP kinase 2 (MK2), a serine/threonine protein kinase with both nuclear and cytoplasmic substrates. One of these substrates is hsp27, a member of the α-crystalline family of small heat shock proteins, and a regulator of filamentous actin and cell contractility (Stokoe *et al*., 1992; Rousseau *et al*., 1997; Schafer *et al*., 1999). We tested whether Ad2 entry required MK2 by evaluating nuclear targeting in mouse MK2 knockout ($MK2^{-/-}$) cells. Wild-type $MK2^{+/+}$ cells efficiently transported Ad2 to the nucleus at 70 min p.i., but $MK2^{-/-}$ cells had significantly lower amounts of perinuclear and nuclear Ad2, and,

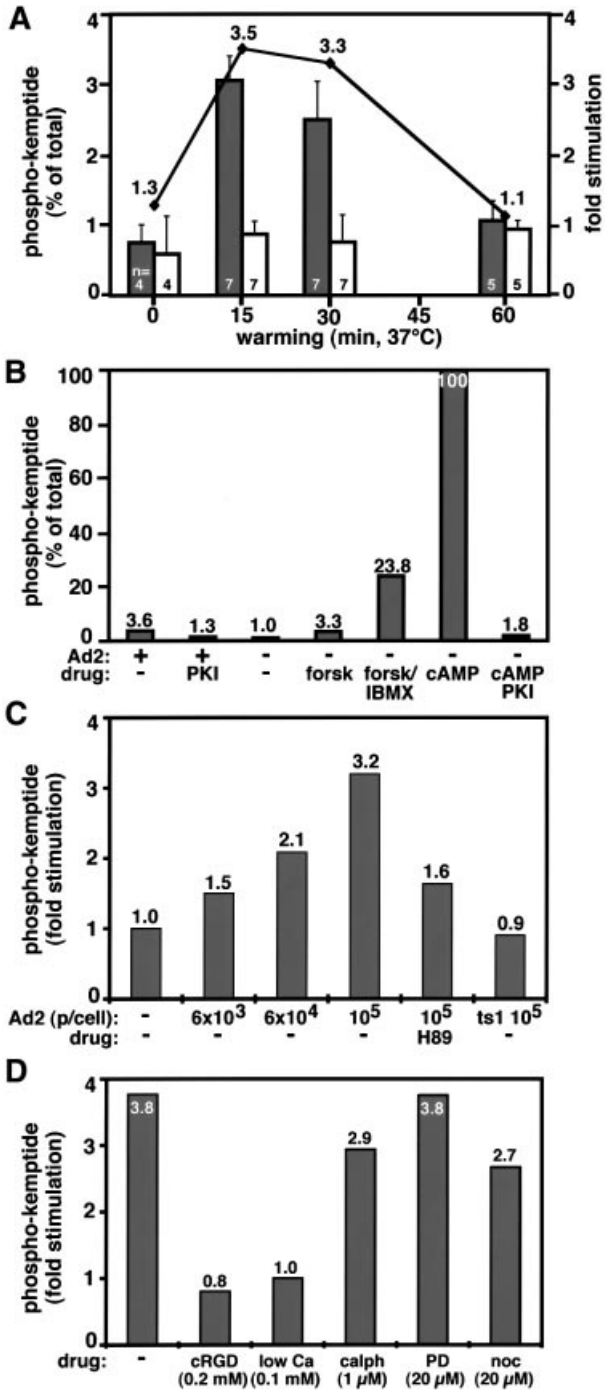

Fig. 3. Transient activation of PKA by incoming Ad2 requires cell surface integrins. Drug-treated or control HeLa cells were incubated in the cold with 6×10^4 Ad2 particles per cell (or as indicated) for 1 h, washed with virus-free medium and warmed up for different times. Kemptide phosphorylations (representing PKA activity) were determined in cell lysates at 15 min p.i. and normalized to the total cAMP-induced kemptide phosphorylations. (**A**) PKA stimulation by Ad2 is transient and peaks at 15 min p.i. Phospho-kemptide amounts are indicated as the mean values (left axis) including the SEM and number of independent experiments (*n*). Fold activation of infected (dark bars) over non-infected (light bars) cells is indicated by the solid line. (**B**) Ad2-stimulated PKA activation amounts to ~3% of the total cellular PKA activity and is comparable to the levels in forskolin-stimulated HeLa cells, which can be boosted by the diesterase inhibitor IBMX. Recombinant PKI added to the cell lysates reduced both Ad2- and cAMP-stimulated kemptide phosphorylations to near background levels. (**C**) PKA activation is dependent on Ad2 particle dose (p/cell) and diminished by pre-incubating cells with the PKA inhibitor H89. The Ad2 mutant ts1 fails to stimulate kemptide phosphorylation. (**D**) cRGD or low-calcium medium, but not the PKC inhibitor calphostin (calph), the MEK inhibitor PD or nocodazole block Ad2-induced kemptide phosphorylation.

instead, increased levels of cytoplasmic and peripheral virus (Figure 4D). Nuclear targeting of Ad2 in MK2$^{-/-}$ cells was rescued by overexpression of hsp27 or hsp27(3D), which mimics phosphorylated hsp27. These results show that four components of the p38 pathway are involved in nuclear targeting of Ad2: MKK6, p38, MK2 and hsp27.

To test whether incoming Ad2 upregulated the p38 pathway, MK2 was immunoprecipitated from infected and non-infected cell lysates and its activity determined using [γ-^{32}P]ATP and a peptidic substrate (KKLNRTLSVA). Infected cells (~4 $\times$ 10^4 Ad2 added per cell) contained up to 3.9-fold higher MK2 activities than non-infected cells (Figure 5A). Elevated activities were first detectable at 15 min, peaked at 30 min and persisted at a 1.5-fold higher level over non-infected cells up to 105 min p.i. Ad2-induced MK2 activity was ~2-fold lower than sorbitol-induced activity (Figure 5A and D). MK2 stimulation was suppressed by fiber knobs, indicating that Ad2 binding to the target cells was required for MK2 activation (not shown). We did not detect MK2 stimulation with the Ad2 mutant ts1 (Figure 5B). This was probably not due to the penetration defect of ts1, since elevated MK2 activities were detected with wild-type Ad2 in cells treated with jasplakinolide (180 nM), an F-actin-stabilizing drug that inhibits Ad2 uptake and penetration (Figure 5C; Nakano *et al*., 2000). As expected, the Ad2-induced stimulation of MK2 was completely inhibited by 10 µM SB, but was only moderately affected by pre-treatment of infected cells with noc or the cell-permeable PKA inhibitor peptide PKI-myr or by the MEK1 inhibitor PD (Figure 5C). MK2 was clearly activated by Ad2 in the presence of cRGD peptides or in low-calcium medium, albeit to somewhat reduced levels compared with control cells (Figure 5C). MK2 activity was not induced by cRGD peptides alone or by the PKA stimulators forskolin or dibuturyl cAMP (dBrcAMP; 0.5 mM), a cell-permeable cAMP analog (Figure 5D). This suggested that MK2 and PKA activations originate from two distinct pathways.

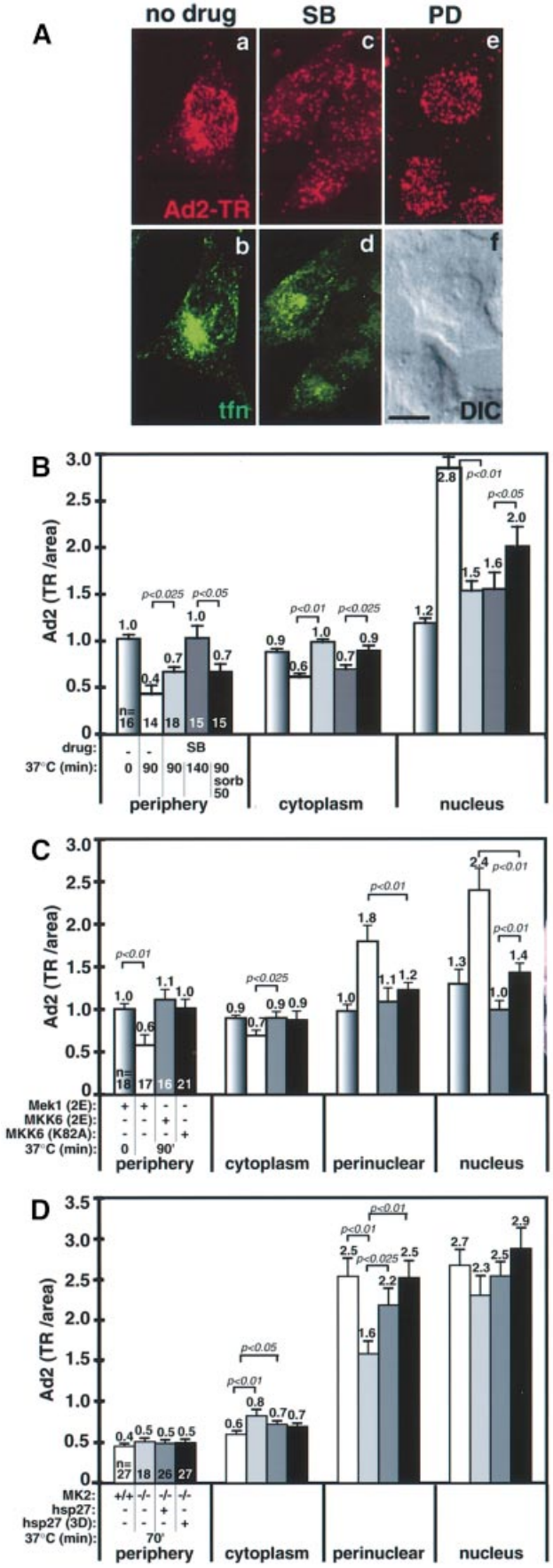

Fig. 4. Nuclear targeting of Ad2 requires MKK6-activated p38 and the downstream p38 targets MK2 and hsp27. (**A**) Control, SB- or PD-treated HeLa cells were infected with Ad2–TR for 70 min (a, c and e, red) in the presence of transferrin–FITC (tfn at 20 µg/ml from 40 to 60 min p.i., b and d), fixed with paraformaldehyde and analyzed by CLSM. Projections of all the optical sections are shown. One corresponding differential interference contrast image (DIC) is shown in (f). Scale bar = 10 µm. (**B**) Quantification of the subcellular localization of Ad2–TR in serum-starved control cells and cells pre-treated with SB (10 µM). HeLa cells were infected with Ad2–TR for 0, 90 or 140 min, followed by washout of SB and subsequent incubation in drug-free medium containing sorbitol (0.4 M). The mean values of TR fluorescence in the cell periphery, the cytoplasm and the nuclear area are indicated, including the SEM, *p* values and the number of cells analyzed. (**C**) Dominant-negative (dn) and constitutively active MKK6 block Ad2 nuclear targeting. HeLa cells were transfected with plasmids encoding constitutively active MKK6 (2E), constitutively active MEK1 (2E) and dn MKK6 (K82A) in the presence of limiting amounts of eGFP plasmid DNA. Ad2–TR fluorescence was quantitated in eGFP-positive cells. (**D**) Quantification of the subcellular localization of Ad2–TR in MK2$^{+/+}$, MK2$^{-/-}$ and MK2$^{-/-}$ cells transfected with plasmids encoding a myc-tagged hsp27 or a myc-tagged hsp27-3D. Cells were infected with Ad2–TR for 70 min, stained for the myc tag using Alexa488-labeled anti-mouse IgG and processed for subcellular analysis of Ad2–TR.

PKA and p38 boost microtubule-dependent minus-end-directed motilities of cytosolic Ad2

We have shown so far that Ad2 infections enhance viral motilities and stimulate PKA and MK2 activities for efficient nuclear targeting of incoming virus. Additional experiments, including quantitative electron microscopy analysis and kinetic uptake measurements, indicated that PKA, p38 and MK2 were not needed for virus delivery to the cytosol (see Supplementary figure 1, available at *The EMBO Journal* Online). To investigate whether these protein kinases regulated motilities of cytosolic Ad2, we performed particle tracking analyses of Ad2–TR in control or inhibitor-treated HeLa cells at 20–60 min p.i., or in mouse MK2$^{-/-}$ and control MK2$^{+/+}$ cells at 30–45 min p.i. (i.e. when virus is in the cytosol). ES were quantitated in terms of directionality and intensity, and results expressed as motility indexes and population velocities. In drug-free HeLa cells, the population velocity (pop. vel.) was directed to the center (–0.57 μm/min) and the motility index was 44% (Figure 6). In contrast, the PKI-myr treated cells transported virus particles towards the periphery (pop. vel. +0.20 μm/min) by inhibiting both the frequencies and extents of the center-directed velocity v_c ($p \leqslant 0.05$). The overall virus motility was also reduced in the absence of PKA ($p < 0.01$). PKI-myr, however, had no effect on the periphery-directed motility v_p. v_p required intact microtubules since combined noc and PKI-myr treatments collapsed the population velocity to –0.05 μm/min, and decreased both the extents and frequencies of center- and periphery-directed motion steps ($p \leqslant 0.01$). To compare lateral motilities under different treatments we calculated the relative lateral motility indexes, defined as $2v_l/(v_c + v_p)$. This index was not affected by PKA inhibition (lateral motility index = 0.74), suggesting that PKA did not suppress lateral motions.

The inhibition of p38 by SB had similar, but not identical effects to the inhibition of PKA (Figure 6). In SB-inhibited cells, v_c was significantly reduced and the net viral movement was directed towards the cell periphery (pop. vel. +0.12 μm/min), despite a reduced overall virus motility (30%, $p < 0.01$) and a slightly reduced periphery-directed velocity (v_p = 0.11 μm/s, $p = 0.05$). Like in the absence of PKA, periphery-directed net movement required intact microtubules, as indicated by combined SB and noc treatments (Figure 6). In these cells, the overall motility was significantly higher than in cells treated with noc alone ($p < 0.01$). This is possibly due to increased lateral motility. Cells lacking both PKA and p38 activities had a near background population velocity (0.05 μm/min) and significantly reduced center- and periphery-directed motility frequencies (Figure 6). The relative lateral motility index increased compared with control cells (1.14), but was similar to that obtained by SB treatment alone. Since inhibition of p38 alone also increased the

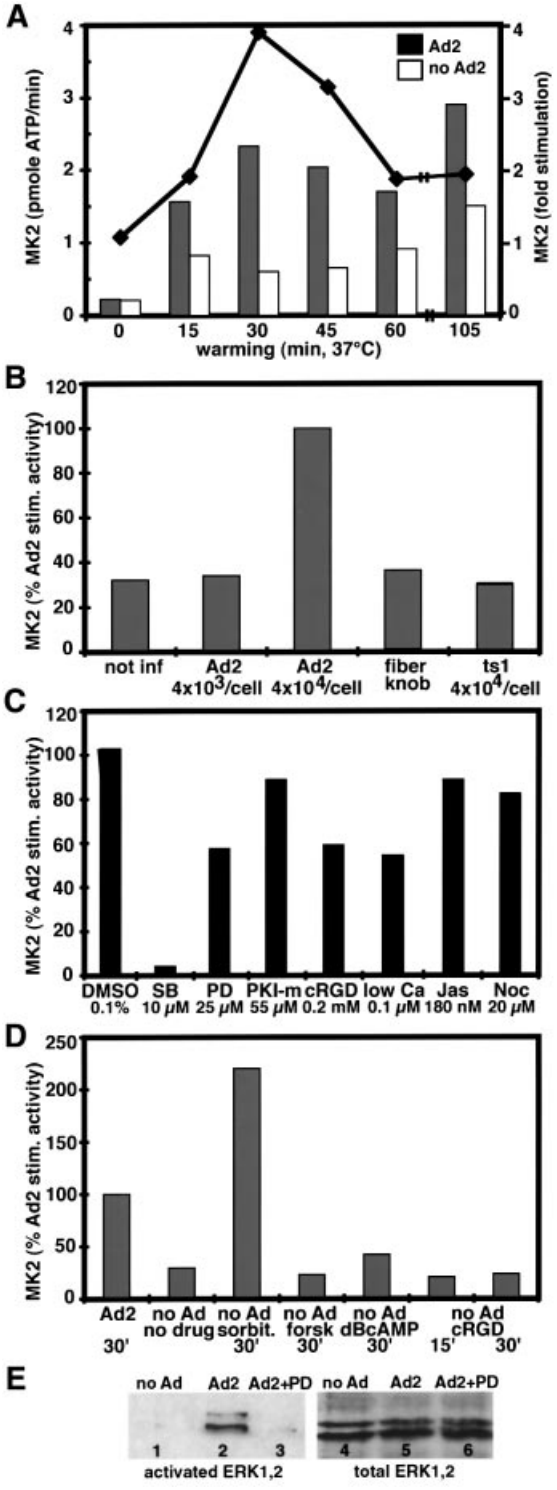

Fig. 5. Transient activation of MK2 by incoming Ad2 originates at the cell surface independent of integrins. Drug-treated or control HeLa cells were incubated in the cold with 4×10^4 Ad2 particles per cell (or as indicated) for 1 h, washed and warmed up for different times. Immunoisolated MK2 activity was determined at 30 min p.i. or as indicated and activity expressed as pmoles of [γ-^{32}P]ATP incorporated/min or fold activation over non-infected cultures. (**A**) MK2 stimulation by Ad2 is transient, peaking at 30 min, and detectable at least up to 105 min p.i. (**B**) Dose-dependent activation of MK2 by wild-type but not the mutant Ad2 ts1. (**C**) MK2 activation is blocked by SB (10 μM), but not by PD (25 μM), PKI-myr (55 μM), cRGD peptides (0.2 mM), low calcium (0.1 μM), jasplakinolide (Jas; 180 nM) or nocodazole (Noc, 20 μM). (**D**) Ad2-induced MK2 activity is in the range of hypertonic stress-induced MK2 activity, but no MK2 induction occurred by forskolin (forsk, 5 μM), dBcAMP (1 μM) or cRGD (0.2 mM) alone. (**E**) Ad2 induces PD-sensitive ERK1,2/MAPK phosphorylations. HeLa cells were treated with or without PD, infected with Ad2 for 15 min, and cell lysates were analyzed for phosphorylated and total ERK1,2 by western blotting.

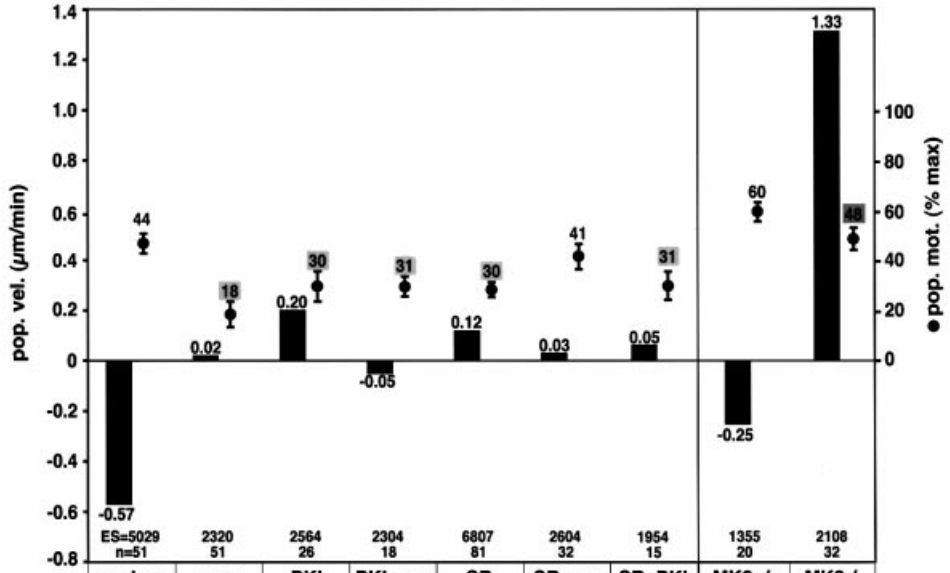

	no drug	noc	PKI	PKI+noc	SB	SB+noc	SB+PKI	MK2+/+	MK2-/-
v_c (μm/s)	-0.15 / 0.01	-0.11 / 0.01	-0.12 / 0.01	-0.09 / 0.01	-0.11 / 0.01	-0.12 / 0.01	-0.10 / 0.01	-0.18 / 0.02	-0.16 / 0.01
v_p (μm/s)	0.13 / 0.01	0.12 / 0.02	0.14 / 0.01	0.09 / 0.01	0.11 / 0.01	0.13 / 0.01	0.10 / 0.01	0.17 / 0.02	0.20 / 0.02
v_l (μm/s)	0.11 / 0.00	0.13 / 0.02	0.10 / 0.00	0.10 / 0.00	0.12 / 0.00	0.13 / 0.00	0.12 / 0.00	0.12 / 0.01	0.11 / 0.01
$2v_l/(v_c+v_p)$	0.74	1.34	0.74	1.13	1.04	1.05	1.14	0.67	0.63
mot c (%)	26 / 2	16 / 4	18 / 3	15 / 2	18 / 2	24 / 2	18 / 3	30 / 3	22 / 2
mot p (%)	23 / 2	15 / 4	21 / 3	14 / 2	21 / 2	22 / 2	19 / 3	30 / 3	30 / 4

Fig. 6. Motility analysis of Ad2–TR in HeLa cells treated with PKA or p38 inhibitors and in $MK2^{+/+}$ and $MK2^{-/-}$ mouse embryo fibroblasts. Ad2–TR was imaged in time-lapse mode and ES analyzed for each particle (*n*) in control or inhibitor-treated HeLa cells at 20–60 min p.i., and in mouse embryo fibroblasts at 30–45 min p.i. Population velocities, population motilities and the average fractions of the vectorial ES components (mot c and mot p) were determined as described in Materials and methods. v_c and v_p (mean/SEM) are the average vectorial velocity components to and from the center for each particle, respectively. v_l depicts the mean lateral vectorial velocity and $2\ v_l/(v_c + v_p)$ is the relative fraction of the average lateral speeds. Light gray (HeLa cells) and dark gray shaded values (mouse MK2 cells) indicate significant differences (p <0.05) to the control HeLa cells (no drug) and $MK2^{+/+}$ cells, respectively. Note that the sum of mot c plus mot p approximates but is not identical to the population motility. Supplementary animation is available at *The EMBO Journal* Online.

lateral motility index, this indicates that in addition to enhancing the overall minus-end-directed viral motility, p38 also suppresses lateral Ad2 motions. This effect was independent of the p38 target MK2, since $MK2^{-/-}$ cells had the same lateral motilities as $MK2^{+/+}$ cells (Figure 6). Like p38-inhibited cells, $MK2^{-/-}$ cells transported virus particles preferentially to the periphery, albeit at higher speed (pop. vel. = 1.33 μm/min compared with –0.25 μm/min for control cells). This was mainly due to a strong decrease in the frequency of minus-end-directed motility steps (p <0.025), and the slightly reduced center-directed and the increased periphery-directed velocities in SB-treated cells. $MK2^{-/-}$ cells had a somewhat reduced overall motility frequency compared with control cells (p = 0.025).

In summary, our results show that PKA, p38 and MK2 activations promote nuclear targeting of Ad2 either by stimulating the frequency and velocity of microtubule-dependent minus-end-directed motility steps or by reducing the velocity of plus-end-directed motilities in the case of p38. Plus-end-directed motility frequencies were only affected by depolymerizing the microtubules, and not by PKA, p38 or MK2 activities.

Discussion

Cytoplasmic motility is crucial for nuclear targeting of incoming viral particles and infections (Sodeik, 2000). Here we show that incoming Ad2 upregulates two distinct cell signaling pathways, which lead to transient activations of PKA and p38/MAPK pathways. Both of these pathways are required for efficient nuclear targeting of infectious Ad2. The signaling events function by tilting the balance of bidirectional microtubule-dependent movements towards the minus ends near the nucleus.

Activation of PKA depends on RGD contacts between Ad2 and an integrin co-receptor, including the $\alpha_v\beta_5$ integrin (Nemerow and Stewart, 1999). The productive engagement of Ad2 with integrins is known to require an intact cortical actin cytoskeleton (Nemerow and Stewart, 1999; Nakano *et al*., 2000). Activation of PKA through integrins has been linked to changes in the actin cytoskeleton and also to mechanical torsions of the plasma membrane (Howe and Juliano, 2000; Meyer *et al*., 2000). It is, therefore, possible that Ad2 activation of PKA involves both integrins and functional F-actin. Although PKA activation roughly coincides with virus uptake, it does not function to facilitate viral endocytosis or escape from endosomes. Instead, it enhances the frequency and extent of microtubule-dependent, minus-end-directed virus transport steps. PKA is not required for plus-end-directed motility of virus, and in PKA-inhibited cells net virus movement is directed towards the cell periphery. Virus in the cell periphery can be rescued by artificial stimulation of PKA using forskolin and IBMX, implying that PKA activation rather than a basal activity is required

to mediate minus-end-directed viral transport. The requirement of activated PKA for efficient minus-end-directed motility of Ad is in marked contrast to regulated movement of pigment granules in melanophores, where activated PKA appears to facilitate the association of kinesin II-bearing granules with microtubules and inhibit microtubule association of cytoplasmic dynein but not dynactin (Reese and Haimo, 2000). Possibly, Ad2 interacts with another kinesin family member that is not subject to PKA regulation. Alternatively, PKA may regulate kinesin and dynein functions through accessory factors or act on only a subset of motor molecules (Okada *et al*., 1995; Reilein *et al*., 1998). Since Ad2- or forskolin-induced PKA stimulations did not detectably affect endosomal transport of transferrin in human (A549, KB, HeLa) or African green monkey kidney cells (TC7; not shown), it is likely that PKA activation by Ad2 specifically enhances minus-end-directed transport of Ad. Further experiments are required to test whether PKA activation globally or locally enhances binding of dynein/dynactin to the viral cargo or the microtubules.

The second pathway activated by incoming Ad2 is integrin- and PKA-independent, and includes p38/MAPK, its upstream activating kinase MKK6 and the p38 target MK2. MK2 activation peaks when most of the viral particles have arrived in the cytosol but not yet at the nucleus. The activated p38 pathway has several motility effects on cytosolic virus, complementing the PKA effects. If p38 is inhibited, both the frequency and the extent of the center-directed speeds are reduced. This is partially explained by lack of MK2 activation, since experiments in $MK2^{-/-}$ cells indicated that MK2 is required for high-frequency minus-end-directed Ad2 motility. In contrast to PKA, which affects both the frequency and extent of minus-end-directed motility, MK2 appears to enhance the probability of dynein/dynactin-mediated transport. This function could be supported by the MK2-target hsp27, since nuclear targeting of Ad2 in $MK2^{-/-}$ cells was rescued by overexpression of hsp27 or the phosphorylation state mimicking mutant hsp27(3D). Since hsp27 affects a variety of processes, including microfilament modulation, cell migration, pinocytosis and also relief of cytotoxic stress (Stokoe *et al*., 1992; Rousseau *et al*., 1997; Schafer *et al*., 1999), its role in the regulation of Ad2 trafficking can be direct or indirect. Further experiments have to show how MK2 and hsp27 are involved in tilting the transport balance towards the nucleus.

p38 also appears to regulate Ad2 motility independently of MK2. Induction of p38 by constitutively active MKK6 (EE207/211) abrogates nuclear targeting of Ad2. Whether this is a direct or indirect effect due to autocrine activation of additional signaling pathways is unknown. Additionally, inhibition of p38 by the chemical SB or by catalytically dead dn MKK6 leads to virus accumulation in the cell periphery. This effect is not seen in $MK2^{-/-}$ cells. It is possible that p38 activation reduces the activity of a plus-end-directed motor, such as kinesin. This possibility was recently suggested for mitochondrial transport to microtubule minus ends in mouse cells stimulated with tissue necrosis factor to induce p38 activation (De Vos *et al*., 2000). However, p38 also appears to regulate microtubule-independent lateral motilities of Ad2. These movements are processive and thus unlikely to be thermally driven Brownian motions. Their relative extent is increased in p38-inhibited or noc-treated cells, but not in MK2-deficient or PKI-treated cells, suggesting that one function of p38 may be to suppress lateral motions and thus enhance nuclear targeting of Ad2.

But why does incoming Ad utilize bidirectional microtubule-dependent transport? Possibly, this motility helps to keep the viral particles on the microtubule tracks and reduces the possibility that the processivity of a particular motor becomes limiting. Such a mechanism might account for the high frequency of overall viral motility, similar to movements of lipid droplets in developing *Drosophila* embryos (Welte *et al*., 1998). A switching mechanism could be subject to PKA, p38, MK2/hsp27 and additional factors controlling the activity of the motors. Such regulations may also depend on the viral structure, as suggested by our observation that the population velocity of microinjected intact Ad2 was directed to the periphery upon signaling by incoming virus, whereas partially uncoated Ad2 was targeted to the nucleus.

Activation of stress responses is typical of viral infections and includes pro-inflammatory signaling leading to tumor necrosis factor-α and IL-6 production in macrophages (Zsengeller *et al*., 2000). Whether, in addition to p38, the Jun N-terminal kinase (JNK) pathway also modulates Ad2 entry is not known. So far, we have failed to detect consistent activation of JNK using antibodies against activated JNK (not shown). The Ad2-activated classical MEK/ERK1,2 pathway, on the other hand, has no impact on the trafficking of the incoming virus particles, but is implicated in the production of the inflammatory cytokine IL-8 (Bruder and Kovesdi, 1997). The Ad2-stimulated PKA and p38 pathways are likely to have nuclear effects as well, including a variety of transcriptional activations such as the phosphorylation of the cAMP-responsive element binding protein CREB (Garrington and Johnson, 1999; Rolli *et al*., 1999). These events might create a favorable nuclear environment for the incoming Ad genome. Interestingly, the p38 pathway was recently linked to the modulation of the splicing preference of the early Ad E1A pre-mRNA (van der Houven van Oordt *et al*., 2000). UV or sorbitol-activated p38 appeared to favor the selection of distal rather than proximal splice sites and thus generated the long 12S and 13S E1A early transcripts, which are necessary to drive viral transcription and replication. In addition to the upregulated PKA and p38/MAPK pathways described here, incoming Ad2 also stimulates PI3K and the small G proteins cdc42 and rac1 to facilitate its endocytic uptake (Nemerow and Stewart, 1999). Thus, different steps in Ad2 entry are highly coordinated by cell signaling. Future studies will explore the possibility that signaling pathways are common regulators of virus entry and may facilitate refining gene delivery protocols and antiviral measures.

Materials and methods

Cells, plasmids, infections and microinjections

Mouse $MK2^{-/-}$ mouse embryo fibroblasts (Kotlyarov *et al*., 1999) and cDNAs encoding dn p38 (A180, 182F) (Raingeaud *et al*., 1996), myc-

tagged wild type and the phosphorylation state mimicking hsp27 mutant 3D (serines 15, 78 and 82 replaced by aspartate residues; Ehrnsperger *et al*., 1999) were generously supplied by M.Gaestel. Catalytically dead dn MKK6 (K82A) and constitutively active MKK6 (S207E, T211E) were obtained from R.Davis (Raingeaud *et al*., 1996), and constitutively active rabbit MEK1 (EE217/221) from S.Zimmermann. Transient transfections were carried out using TransFast™ (Promega, Catalys, Switzerland) in the presence of limiting amounts of eGFP–DNA (InVitroGen, The Netherlands) and cells analyzed 24 h later. Preparations and microinjections of viruses were as described (Nakano and Greber, 2000).

Proteins and chemicals

Recombinant fiber knob was purified to homogeneity from baculovirus-infected Schneider cells (Louis *et al*., 1994). Anti-lamin A,B,C antibody (rabbit 8188) was kindly supplied by L.Gerace and mouse monoclonal anti-tyrosinated α-tubulin antibody 1A2 was obtained from T.Kreis. Rabbit anti-ERK1,2 (total p44/42) and monoclonal anti-phospho-ERK1,2 antibodies were from New England Biolabs (BioConcept, Switzerland) and Sigma, respectively. The mouse anti-c-myc tag antibody 9E10 was purchased from Sigma, and fluorescein isothiocyanate (FITC)-labeled human transferrin and goat anti-mouse IgG–Alexa488 from Molecular Probes (Leiden, The Netherlands). cRGD peptides and NLS peptides (CGYGPKKKRKVED) were synthesized by the Yale peptide facility (New Haven, CT). H-89, KT5720, IBMX, myristoylated PKIα (amino acids 14–22, PKI-myr), recombinant PKIα (PKI), myristoylated autocamptide, calphostin, PD, SB and SB202474 were purchased from Calbiochem (Juro Supplies AG, Switzerland), and cAMP (free acid), dBcAMP, forskolin, noc and sorbitol were from Sigma (Fluka, Switzerland). For inhibitor experiments, cells were pre-incubated with drugs at 37°C for 30 min and drugs kept present throughout virus binding and internalization.

In vitro PKA and MK2 kinase assays

PKA activity was assayed in crude cell lysates using the peptidic substrate kemptide (LRRASLG; one-letter amino acid sequence code, porcine liver pyruvate kinase, Bachem AG, Switzerland; Jans and Hemmings, 1991). Briefly, duplicate 30 mm plates of parallel infected and non-infected cells were lysed in a buffer containing 20 mM 2-[*N*-morpholino] ethane sulfonic acid (MES)–NaOH pH 6.9, 150 mM NaCl, 1 mM EDTA, 0.2% Triton X-100 on ice for 8 min. Insoluble material was removed by a 4 min full-speed centrifugation in an Eppendorf centrifuge at 4°C; supernatants of parallel samples were pooled and duplicate aliquots of the supernatants were assayed for kemptide phosphorylation activity in a reaction mixture containing 53 mM MES–NaOH pH 6.9, 56 mM NaCl, 0.4 mM EDTA, 3 mM magnesium acetate, 1.3 mg/ml bovine serum albumin, 0.1 mg/ml kemptide, 0.1 mM ATP, ~1 μCi [γ-^{32}P]ATP per assay. Samples were incubated at 30°C for 15 min and reactions stopped by spotting the liquid onto Whatman P81 filter papers. Filters were immersed and washed in 0.5% phosphoric acid, air-dried and radioactivity determined by liquid scintillation counting using Ready-Safe (Beckman Instruments). Background values of reactions lacking kemptide were subtracted from all values, and activities calculated as picomoles of ATP incorporated into kemptide/min/mg of protein. Results were expressed as a percentage of total PKA activity in cell extracts determined in the presence of cAMP (11 μM). The sensitivity of kemptide phosphorylations to the PKA inhibitor PKI was determined by including the full-length recombinant PKI (0.1 U/μl; Calbiochem) in the assay mixture. The protein concentration in cell lysates was determined using the DC assay kit (BioRad).

MK2 kinase activity was determined in immunocomplexes of lysates from infected and parallel non-infected cells using an acceptor peptide (KKLNRTLSVA; Upstate Biotechnology) and [γ-^{32}P]ATP as indicated by the MK2 antibody supplier (Upstate Biotechnology, Lucerna AG, Switzerland). Background values obtained from reactions lacking the acceptor peptide were subtracted from all values. Kinase activity was expressed as picomoles of ATP incorporated into the acceptor peptide/min or, alternatively, as fold stimulation compared with the activity in parallel non-infected cells.

Activation of ERK1,2

Serum-starved HeLa cells were treated with or without PD, incubated with Ad2 in the cold, washed and warmed for 15 min in the presence or absence of PD. Cells were lysed with cold lysis buffer (20 mM Tris–HCl pH 8.0, 10 mM EGTA, 1% Triton X-100, 0.5% deoxycholate, 40 mM sodium pyrophosphate, 50 mM NaF, 5 mM $MgCl_2$, 100 μM orthovanadate, 25 mM sodium glycerophosphate, 0.1 μM okadaic acid, 1 mM phenylmethylsulfonyl fluoride, 1 μg/ml CLAP). Insoluble material was removed by centrifugation at 10 000 *g* at 4°C, and supernatants were analyzed directly by SDS–PAGE and western blotting using monoclonal anti-active ERK1,2 antibody or rabbit anti-total ERK1,2 followed by goat anti-mouse–horseradish peroxidase (HRP) and goat anti-rabbit–HRP (Sigma, Fluka, Switzerland).

Viral motilities, microscopy and entry

Live data were acquired by a back-illuminated CCD camera (Princeton Instruments) using the MetaMorph software package (Universal Imaging Corp., Visitron GmBH, Germany) and computed with Excel software (Microsoft Corp., USA) as described (Suomalainen *et al*., 1999; Nakano and Greber, 2000). Virus particles that underwent at least three ES >0.1 μm/s during the sampling period of 1–2 min were randomly selected for analysis. ES <0.1 μm/s were below the resolution of our tracking system and were scored as 'no motility'. Population velocities were calculated from the net distance traveled to and from the nucleus divided by the total time of sampling of the analyzed particles (*n*). Population motilities represented the mean number of ES >0.1 μm/s divided by the total number of ES of each particle. v_c, v_p and v_l were defined as the average vectorial velocity components to the center, the periphery and to lateral sides, respectively. mot c and mot p were defined as the average fractions of the vectorial ES components >0.1 μm/s directed towards the center (c) or the periphery (p), including the SEM. *p* values were determined using one-sided *t*-tests. Quantifications of Ad2–TR in subcellular regions of fixed cells, CLSM and fluorescence *in situ* hybridizations (FISH) were performed as described (Suomalainen *et al*., 1999; Nakano and Greber, 2000). Internalization of [^{35}S]methionine-labeled Ad2 into KT5720 (5 μM) or SB (20 μM) treated cells was carried out as described (Greber *et al*., 1993). Ad2 localization at the plasma membrane, in endocytic vesicles and the cytosol of subconfluent control, PKI-myr (55 μM) or SB (20 μM) treated cells was determined by quantitative electron microscopy (Nakano *et al*., 2000).

Supplementary data

Supplementary data for this paper are available at *The EMBO Journal* Online.

Acknowledgements

We thank Robert Stidwill for help with CLSM data acquisition and discussions, Matthias Gaestel and Jadwiga Chrobozcek for cell lines, cDNAs and viruses, and Brian Hemmings, Ernst Hafen and members of the Greber laboratory for helpful discussions. This work was supported by an EMBO long-term fellowship (to M.S.), a grant from the Swiss National Science Foundation (to U.F.G.) and the Kanton of Zürich.

References

Alessi,D.R., Cuenda,A., Cohen,P., Dudley,D.T. and Saltiel,A.R. (1995) PD 098059 is a specific inhibitor of the activation of mitogen-activated protein kinase kinase *in vitro* and *in vivo*. *J. Biol. Chem.*, **270**, 27489–27494.

Bergelson,J.M., Cunningham,J.A., Droguett,G., Kurt-Jones,E.A., Krithivas,A., Hong,J.S., Horwitz,M.S., Crowell,R.L. and Finberg, R.W. (1997) Isolation of a common receptor for Coxsackie B viruses and adenoviruses 2 and 5. *Science*, **275**, 1320–1323.

Beyaert,R., Cuenda,A., Vanden Berghe,W., Plaisance,S., Lee,J.C., Haegeman,G., Cohen,P. and Fiers,W. (1996) The p38/RK mitogen-activated protein kinase pathway regulates interleukin-6 synthesis response to tumor necrosis factor. *EMBO J.*, **15**, 1914–1923.

Bruder,J.T. and Kovesdi,I. (1997) Adenovirus infection stimulates the Raf/Mapk signaling pathway and induces interleukin-8 expression. *J. Virol.*, **71**, 398–404.

De Vos,K., Severin,F., Van Herreweghe,F., Vancompernolle,K., Goossens,V., Hyman,A. and Grooten,J. (2000) Tumor necrosis factor induces hyperphosphorylation of kinesin light chain and inhibits kinesin-mediated transport of mitochondria. *J. Cell Biol.*, **149**, 1207–1214.

Dramsi,S. and Cossart,P. (1998) Intracellular pathogens and the cytoskeleton. *Annu. Rev. Cell Dev. Biol.*, **14**, 137–166.

Ehrnsperger,M., Lilie,H., Gaestel,M. and Buchner,J. (1999) The dynamics of Hsp25 quaternary structure. Structure and function of different oligomeric species. *J. Biol. Chem.*, **274**, 14867–14874.

Frischknecht,F., Moreau,V., Rottger,S., Gonfloni,S., Reckmann,I., Superti-Furga,G. and Way,M. (1999) Actin-based motility of

vaccinia virus mimics receptor tyrosine kinase signalling. *Nature*, **401**, 926–929.

Gamm,D.M. and Uhler,M.D. (1995) Isoform-specific differences in the potencies of murine protein kinase inhibitors are due to nonconserved amino-terminal residues. *J. Biol. Chem.*, **270**, 7227–7232.

Garrington,T.P. and Johnson,G.L. (1999) Organization and regulation of mitogen-activated protein kinase signaling pathways. *Curr. Opin. Cell Biol.*, **11**, 211–218.

Greber,U.F., Willetts,M., Webster,P. and Helenius,A. (1993) Stepwise dismantling of adenovirus 2 during entry into cells. *Cell*, **75**, 477–486.

Greber,U.F., Suomalainen,M., Stidwill,R.P., Boucke,K., Ebersold,M. and Helenius,A. (1997) The role of the nuclear pore complex in adenovirus DNA entry. *EMBO J.*, **16**, 5998–6007.

Griego,S.D., Weston,C.B., Adams,J.L., Tal-Singer,R. and Dillon,S.B. (2000) Role of p38 mitogen-activated protein kinase in rhinovirus-induced cytokine production by bronchial epithelial cells. *J. Immunol.*, **165**, 5211–5220.

Howe,A.K. and Juliano,R.L. (2000) Regulation of anchorage-dependent signal transduction by protein kinase A and p21-activated kinase. *Nature Cell Biol.*, **2**, 593–600.

Jacque,J.M., Mann,A., Enslen,H., Sharova,N., Brichacek,B., Davis,R.J. and Stevenson,M. (1998) Modulation of HIV-1 infectivity by MAPK, a virion-associated kinase. *EMBO J.*, **17**, 2607–2618.

Jans,D.A. and Hemmings,B.A. (1991) cAMP-dependent protein kinase activation affects vasopressin V2-receptor number and internalization in LLC-PK1 renal epithelial cells. *FEBS Lett.*, **281**, 267–271.

Kotlyarov,A., Neininger,A., Schubert,C., Eckert,R., Birchmeier,C., Volk,H.D. and Gaestel,M. (1999) MAPKAP kinase 2 is essential for LPS-induced TNF-α biosynthesis. *Nature Cell Biol.*, **1**, 94–97.

Krijnse Locker,J., Kuehn,A., Schleich,S., Rutter,G., Hohenberg,H., Wepf,R. and Griffiths,G. (2000) Entry of the two infectious forms of vaccinia virus at the plasma membane is signaling-dependent for the IMV but not the EEV. *Mol. Biol. Cell*, **11**, 2497–2511.

Lee,J.C. *et al*. (1994) A protein kinase involved in the regulation of inflammatory cytokine biosynthesis. *Nature*, **372**, 739–746.

Leopold,P.L., Kreitzer,G., Miyazawa,N., Rempel,S., Pfister,K.K., Rodriguez-Boulan,E. and Crystal,R.G. (2000) Dynein- and microtubule-mediated translocation of adenovirus serotype 5 occurs after endosomal lysis. *Hum. Gene Ther.*, **11**, 151–165.

Louis,N., Fender,P., Barge,A., Kitts,P. and Chroboczek,J. (1994) Cell-binding domain of adenovirus serotype 2 fiber. *J. Virol.*, **68**, 4104–4106.

Meyer,C.J., Alenghat,F.J., Rim,P., Fong,J.H., Fabry,B. and Ingber,D.E. (2000) Mechanical control of cyclic AMP signalling and gene transcription through integrins. *Nature Cell Biol.*, **2**, 666–668.

Miller,W.E. and Raab-Traub,N. (1999) The EGFR as a target for viral oncoproteins. *Trends Microbiol.*, **7**, 453–458.

Nagata,K., Puls,A., Futter,G., Aspenstrom,P., Schaefer,E., Nakata,T., Hirokawa,N. and Hall,A. (1998) The MAP kinase kinase kinase Mlk2 co-localizes with activated Jnk along microtubules and associates with kinesin superfamily motor Kif3. *EMBO J.*, **17**, 149–158.

Nakano,M.Y. and Greber,U.F. (2000) Quantitative microscopy of fluorescent adenovirus entry. *J. Struct. Biol.*, **129**, 57–68.

Nakano,M.Y., Boucke,K., Suomalainen,M., Stidwill,R.P. and Greber, U.F. (2000) The first step of adenovirus type 2 disassembly occurs at the cell surface, independently of endocytosis and escape to the cytosol. *J. Virol.*, **74**, 7085–7095.

Nemerow,G.R. and Stewart,P.L. (1999) Role of α(v) integrins in adenovirus cell entry and gene delivery. *Microbiol. Mol. Biol. Rev.*, **63**, 725–734.

Okada,Y., Sato-Yoshitake,R. and Hirokawa,N. (1995) The activation of protein kinase A pathway selectively inhibits anterograde axonal transport of vesicles but not mitochondria transport or retrograde transport *in vivo*. *J. Neurosci.*, **15**, 3053–3064.

Pelchen-Matthews,A., Signoret,N., Klasse,P.J., Fraile-Ramos,A. and Marsh,M. (1999) Chemokine receptor trafficking and viral replication. *Immunol. Rev.*, **168**, 33–49.

Raingeaud,J., Whitmarsh,A.J., Barrett,T., Derijard,B. and Davis,R.J. (1996) MKK3- and MKK6-regulated gene expression is mediated by the p38 mitogen-activated protein kinase signal transduction pathway. *Mol. Cell. Biol.*, **16**, 1247–1255.

Reese,E.L. and Haimo,L.T. (2000) Dynein, dynactin and kinesin II's interaction with microtubules is regulated during bidirectional organelle transport. *J. Cell Biol.*, **151**, 155–166.

Reilein,A.R., Tint,I.S., Peunova,N.I., Enikolopov,G.N. and Gelfand,V.I. (1998) Regulation of organelle movement in melanophores by protein kinase A (PKA), protein kinase C (PKC) and protein phosphatase 2A (PP2A). *J. Cell Biol.*, **142**, 803–813.

Rolli,M., Kotlyarov,A., Sakamoto,K.M., Gaestel,M. and Neininger,A. (1999) Stress-induced stimulation of early growth response gene-1 by p38/stress-activated protein kinase 2 is mediated by a cAMP-responsive promoter element in a MAPKAP kinase 2-independent manner. *J. Biol. Chem.*, **274**, 19559–19564.

Rousseau,S., Houle,F., Landry,J. and Huot,J. (1997) p38 MAP kinase activation by vascular endothelial growth factor mediates actin reorganization and cell migration in human endothelial cells. *Oncogene*, **15**, 2169–2177.

Schafer,C., Clapp,P., Welsh,M.J., Benndorf,R. and Williams,J.A. (1999) HSP27 expression regulates CCK-induced changes of the actin cytoskeleton in CHO-CCK-A cells. *Am. J. Physiol.*, **277**, C1032–1043.

Sheetz,M.P. (1999) Motor and cargo interactions. *Eur. J. Biochem.*, **262**, 19–25.

Sodeik,B. (2000) Mechanisms of viral transport in the cytoplasm. *Trends Microbiol.*, **8**, 465–472.

Stokoe,D., Engel,K., Campbell,D.G., Cohen,P. and Gaestel,M. (1992) Identification of MAPKAP kinase 2 as a major enzyme responsible for the phosphorylation of the small mammalian heat shock proteins. *FEBS Lett.*, **313**, 307–313.

Suomalainen,M., Nakano,M.Y., Boucke,K., Keller,S., Stidwill,R.P. and Greber,U.F. (1999) Microtubule-dependent minus and plus end-directed motilities are competing processes for nuclear targeting of adenovirus. *J. Cell Biol.*, **144**, 657–672.

Tang,H., Kuhen,K.L. and Wong-Staal,F. (1999) Lentivirus replication and regulation. *Annu. Rev. Genet.*, **33**, 133–170.

van der Houven van Oordt,W., Diaz-Meco,M.T., Lozano,J., Krainer, A.R., Moscat,J. and Caceres,J.F. (2000) The MKK(3/6)-p38-signaling cascade alters the subcellular distribution of hnRNP A1 and modulates alternative splicing regulation. *J. Cell Biol.*, **149**, 307–316.

Wallach,D., Varfolomeev,E.E., Malinin,N.L., Goltsev,Y.V., Kovalenko, A.V. and Boldin,M.P. (1999) Tumor necrosis factor receptor and Fas signaling mechanisms. *Annu. Rev. Immunol.*, **17**, 331–367.

Wang,X.H. and Bergelson,J.M. (1999) Coxsackievirus and adenovirus receptor cytoplasmic and transmembrane domains are not essential for Coxsackievirus and adenovirus infection. *J. Virol.*, **73**, 2559–2562.

Welte,M.A., Gross,S.P., Postner,M., Block,S.M. and Wieschaus,E.F. (1998) Developmental regulation of vesicle transport in *Drosophila* embryos—forces and kinetics. *Cell*, **92**, 547–557.

Zsengeller,Z., Otake,K., Hossain,S.A., Berclaz,P.Y. and Trapnell,B.C. (2000) Internalization of adenovirus by alveolar macrophages initiates early proinflammatory signaling during acute respiratory tract infection. *J. Virol.*, **74**, 9655–9667.

Received November 2, 2000; revised January 11, 2001; accepted January 23, 2001